Extended Alcohol Catalytic Chemical Vapor Deposition for Efficient Growth of Single-walled Carbon Nanotubes Thinner than (6,5)

Bo Hou,[†] *Cheng Wu,*[‡] *Taiki Inoue,*[‡] *Shohei Chiashi,*[‡] *Rong Xiang,*[‡] *and Shigeo Maruyama*[†,]

[‡]*

[†] Energy NanoEngineering Lab., Department of Energy and Environment, AIST, Tsukuba 305-8564, Japan

[‡]Department of Mechanical Engineering, The University of Tokyo, Tokyo 113-8656, Japan

∗ Address correspondence to

maruyama@photon.t.u-tokyo.ac.jp

xiangrong@photon.t.u-tokyo.ac.jp

ABSTRACT

We performed a comprehensive exploration on alcohol catalytic chemical vapor deposition (ACCVD) synthesis of single-walled carbon nanotubes (SWCNTs), and with more than 70 temperature-pressure sets, we presented an extended ACCVD parametric map that covers a wide range of temperature from 340 to 950°C and a wide pressure range over 6 orders of magnitude. Efficient synthesis of high quality SWCNTs becomes possible at temperatures down to 400 °C and pressure as low as 10^{-2} Pa, which is benefited from the strong correlation between temperature and pressure newly discovered in this exploration. The underlying mechanism is clarified through a kinetic model, and two growth boundaries on the extended experimental map are explained by a transfer-free TEM observation. Most importantly, after extending growth window of ACCVD, successful synthesis at extreme low temperature and pressure gives a significantly enhanced yield for super-small diameter SWCNTs (0.8 nm > d_t > 0.62 nm) thinner than (6, 5) that are rarely observed from direct synthesis.

TOC Graphic
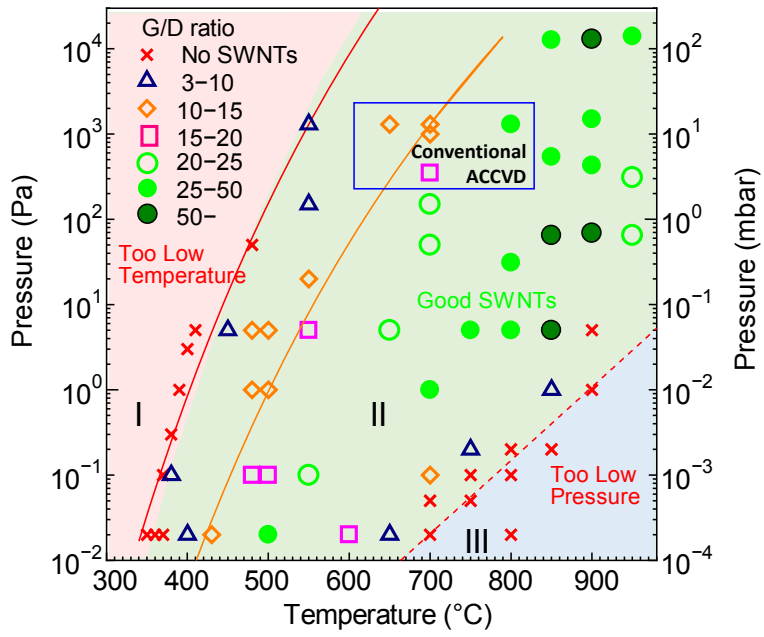
1. Introduction

Single-walled carbon nanotubes (SWCNTs), a unique one-dimensional structure of a rolled-up graphene sheet, have become one of the central topics in nano-technology research in the past few decades due to their outstanding mechanical, thermal, optical and electronic properties.[1] Great efforts have been made to optimize the synthesis of SWCNTs.[2-4] Up to date, Arc discharge,[5] laser ablation[6] and chemical vapor deposition (CVD)[7-9] have been proposed for SWCNTs production. In particular, CVD possesses advantages in low-cost, scalability and has become one of the main methods for SWCNT production in both laboratory and industrial scale.

In 2002,[10] we discovered the growth of clean and high-quality SWCNTs by alcohol catalytic chemical vapor deposition (ACCVD). As an efficient method, ACCVD has been wildly used to synthesis SWCNTs in various morphologies, including random SWCNTs on zeolite support, world-first vertically aligned array forest,[11, 12] and horizontally aligned SWCNT arrays.[13, 14] These ACCVD produced SWCNTs are highly tunable in length, diameter, chirality range, and achieved good performances in thin film transistors and solar cell.[15-17]

Even harvest improvements were achieved in the field of growth of SWCNTs, we still face the challenges of controlling growth and freely tuning the structure of SWCNTs. Also, CVD growth of SWCNTs is usually performed in a narrow parameter window. For example, in previous ACCVD, efficient growth of SWCNTs was experimentally observed only from 600°C to 800°C and at a constant pressure around 1 kPa.[18, 19] Moreover, this narrow parameter window is not always compatible to other processes that uses more severe conditions (e.g., MEMS techniques usually require a low working temperature, and *in situ* TEM studies need a very low pressure inside TEM column). Therefore, extending the growth window of ACCVD can not only improve the

process robustness of ACCVD and the controllability over the product, but may also provide a path to a better understanding on growth mechanism of SWCNTs.

In this work, extended temperature from 350°C to 950°C, coupled pressure with 6 orders of magnitude were systematically varied for growth of SWCNTs in ACCVD on zeolite support Fe-Co catalyst (simplified as extended ACCVD hereafter). Extended working window implies a chance to efficient growth of SWCNTs which are not preferably formed in conventional ACCVD. After optimizing the low temperature growth condition, super-small diameter SWCNTs thinner than (6,5), such as (6,4), has been grown with the so far highest yield, as solidly confirmed by various characterizations. Also, a strong relationship between temperature and pressure is identified. Effect of temperature and pressure on the quality, mean diameter, and diameter distribution of SWCNTs reveals an update understanding for growth mechanism in extended ACCVD system.

2. Experimental

Zeolite support catalyst carried by a quartz boat is set in a quartz tube (i.d. 27 mm) inside an electric furnace as shown in Fig. S1. During heating to target temperature by the electric furnace, 300 sccm (standard cc/min) of Ar/H_2 (3% H_2) is employed so as to maintain the pressure inside the quartz tube at 40 ± 1 kPa. The quartz tube is evacuated by a rotary pump after the electric furnace reached the growth temperature, and at the same time Ar/H_2 is stopped. Ethanol vapor from a reservoir with carrier gas Ar (500 sccm) are then introduced at a constant pressure. After completion of the CVD reaction, carbon source is stopped, then the tube is cooled down to room temperature with flow gas (Ar or Ar/H_2) through the tube. Growth temperature was varied between 350ºC and 900ºC, and growth pressure (partial pressure of ethanol in the work unless otherwise

stated) was between 0.02 Pa and 15 kPa. After cooling down, as-grown SWCNTs sample in the quartz boat was took out for characterizations. More details of the catalyst preparation process and CVD parameters can be found in our previous reports. [10, 11, 20, 21] The Raman spectra are measured on as-grown samples (without any post-treatments) by Renishaw inVia Raman Microscope using 5 lasers of 488 nm, 532 nm, 633 nm, 785 nm and l064 nm. SEM (S-4800, Hitachi Co.,Ltd.) and TEM (TEM, JEOL 2000EX) are used to observe the morphology of as-grown SWCNTs directly. UV-vis-NIR absorption and photoluminescence excitation of dispersed SWCNTs solution are measured through UV-3150, (Shimadzu Co., Ltd.) and HORIBA Jobin Yvon Fluorolog iHR320 with a liquid-nitrogen-cooled GaAs detector respectively.

3. Results and discussion

3.1 Characterization of high quality SWCNTs grown in extended temperature range

Efficient growth of SWCNTs in extended ACCVD over a wide temperature and pressure range and characterizations of the product using various techniques (Fig. 1-3) are demonstrated in this section. Different from our previous studies, the ethanol pressure is kept at 5 Pa, which is nearly three orders of magnitude lower. This low pressure is found to be critical for the successful growth of SWCNTs in extended temperature ranges, as to be discussed in detail later. Fig. 1 shows Raman spectra of SWCNTs grown at different temperatures using 5 Pa ethanol. All samples have G/D ratio over 15, suggesting the produced SWCNTs are well crystalized. In our previous studies using high pressure of ethanol, SWCNTs are usually defective with a G/D around two to three when temperature is lower than 600°C. However, in this study, even temperature decrease to 500°C, we still obtain SWCNTs with very high quality. RBM region clearly confirms the existence of many SWCNTs in the whole temperature range. One general trend is super-small diameter SWCNTs (d_t

< 1 nm) are obtained when temperature is down to 550°C, which is clearly evidence by the appearance of high frequency modes in Raman shift in RBM regions. In Fig. 2, chirality of dispersed SWCNTs are identified in the PL maps. (6,5) becomes dominant when growth temperature is lower than 550°C, whereas (7,5) is dominant when growth temperature is higher than 650°C. Growth of (6,4) is efficiently enhanced when temperature is lower than 550°C, which is also consistently observed by absorption spectroscopy shown in Fig. 3.
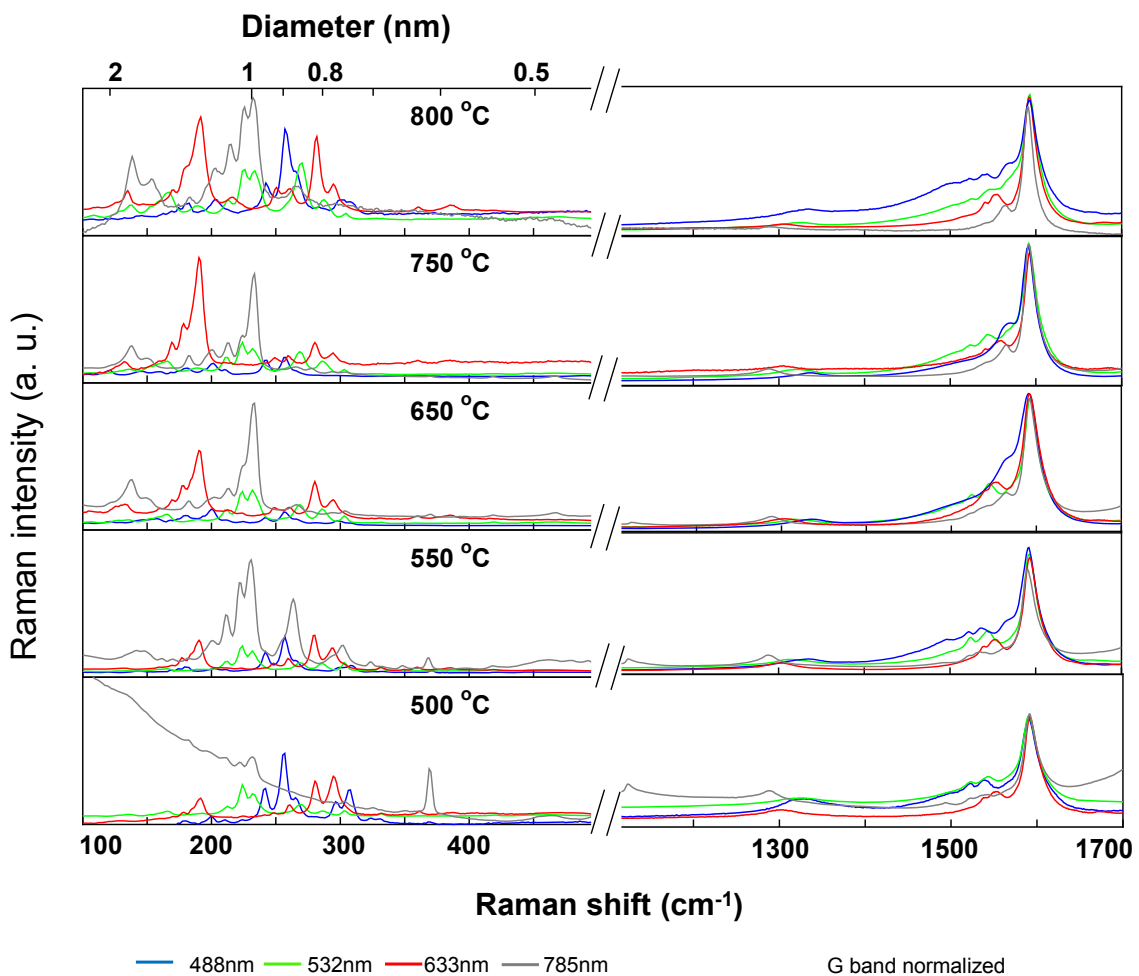

Figure 1. Raman spectra of SWCNTs grown from 800°C to 500°C at 5 Pa, presenting differences in the RBM region and D-band caused by different chirality and quality of SWCNTs at different temperatures.
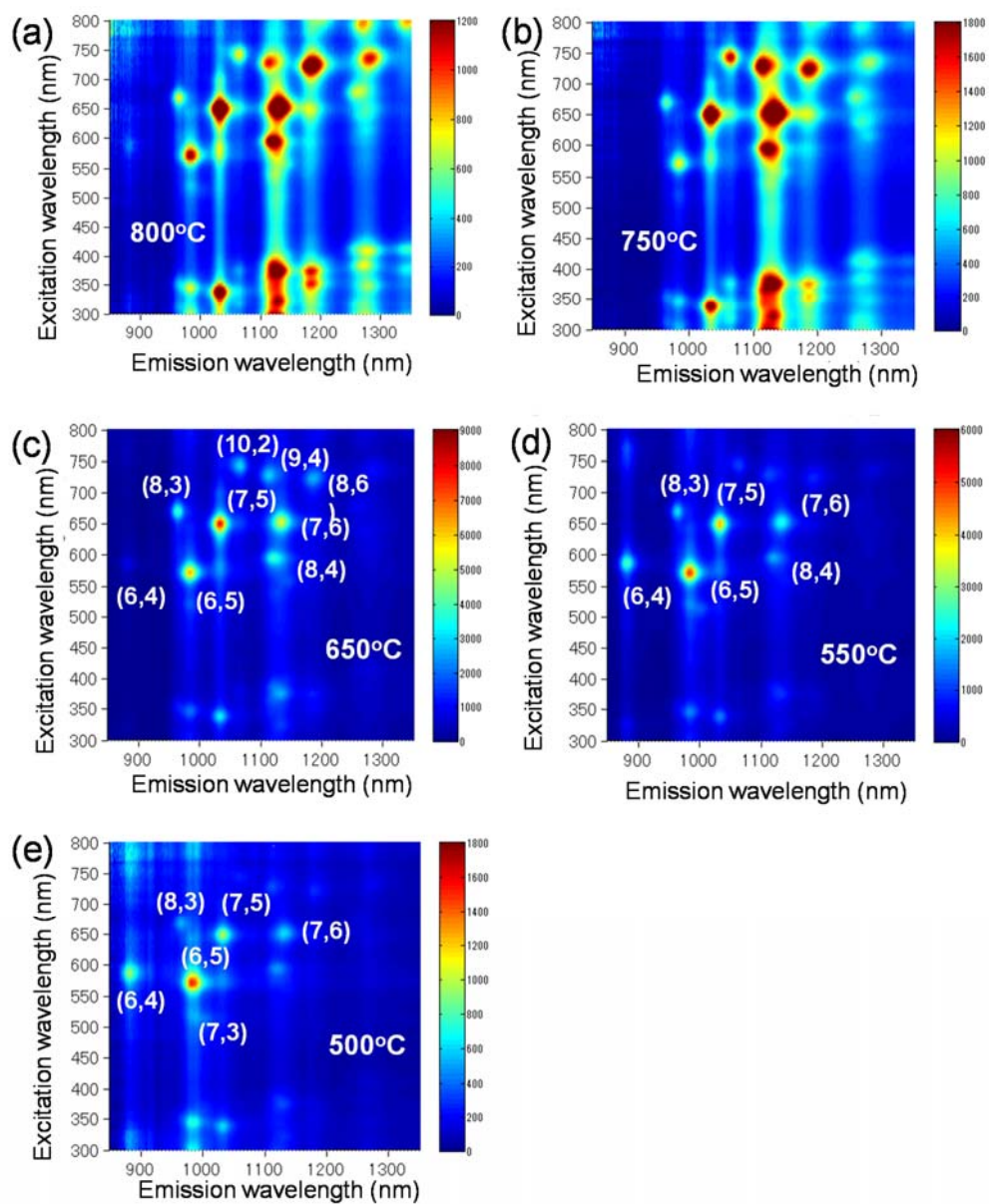
Figure 2. PL mappings of dispersed SWCNTs grown from 800°C to 500°C at an ethanol pressure of 5 Pa.
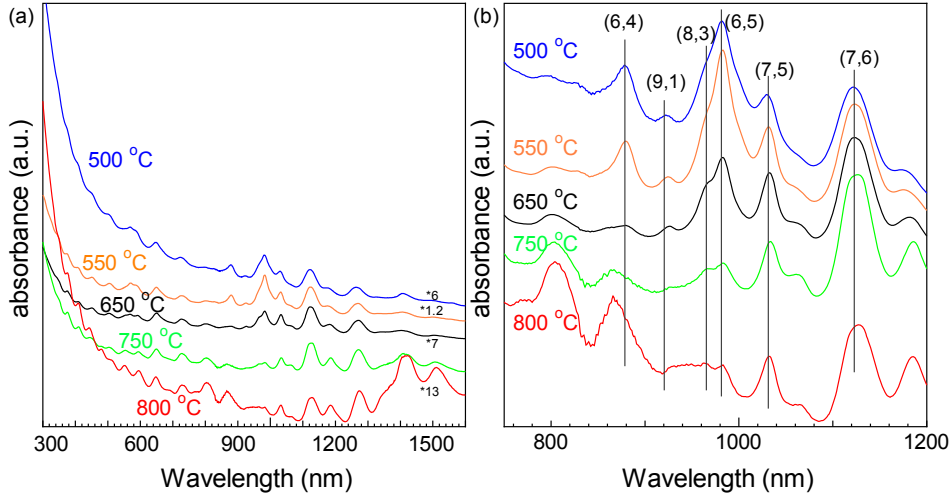
Figure 3. (a) UV-vis-NIR optical absorption spectra of SWCNTs from 800°C to 500°C at 5 Pa, and (b) expanded E_{11}^s region of absorption spectra showing chirality of SWCNTs.

As a pressure of 5 Pa allows growth of high quality SWCNTs at low temperature, we further decrease the pressure to confirm the correlation between pressure and temperature of CVD. Fig. 4a shows Raman spectra of SWCNTs grown at different pressures using 480°C, pressure strongly affect the G/D ratio and diameter distribution, which will be specifically discussed later. To track the changes of SWCNTs growth along the boundary conditions, SWCNTs obtained from 370°C to 700°C at 0.02 Pa (0.02 Pa is the lowest pressure in this work) are observed by Raman spectroscopy with excitation energy laser 532 nm. As shown in Fig. 4b, SWCNTs can be synthesized from 400°C to 650°C at 0.02 Pa, neither 370°C nor 700°C can grow SWCNTs, which indicates that optimal CVD temperature decreased when a lower pressure is used.
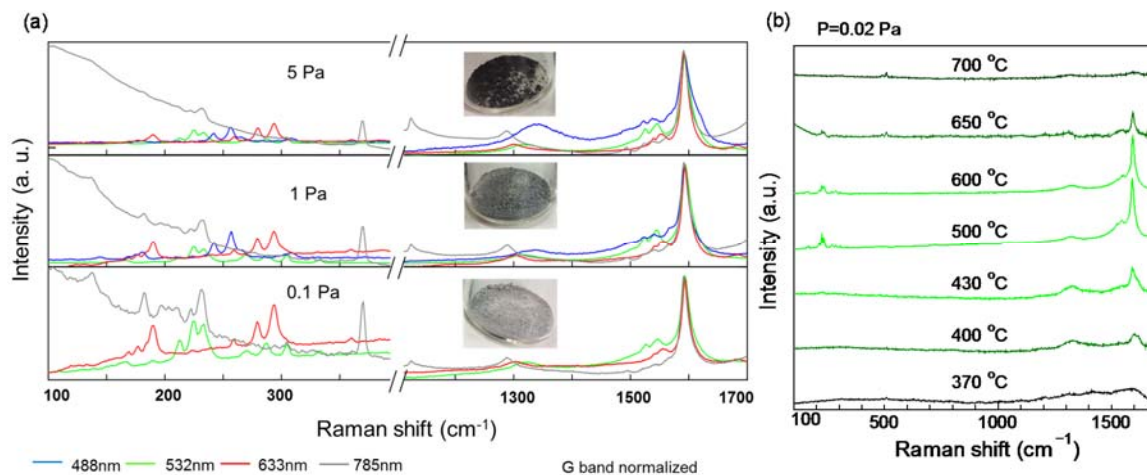
9

Figure 4. (a) Raman spectra of SWCNTs growth from 0.1 Pa to 5 Pa at 480°C by four excitation energy lasers. (b) Raman spectra (λ=532 nm) of samples grown from 370°C to 700°C at an ethanol pressure of 0.02 Pa, suggesting the growth boundary and optimal growth temperature.

3.2 Correlation between temperature and pressure in full parametric map of extended ACCVD

In previous ACCVD at an ethanol pressure around 1 kPa, it is difficult to grow and optically observe the SWCNTs when growth temperature is lower than 600°C. In this work, however, efficient growth of high quality SWCNTS can be extended to 500°C as long as ethanol pressure is decreased to 5 Pa, and can be extended to 430°C when the pressure is decreased to 0.02 Pa. The yield of SWNTs (percentage of SWNTs over catalyst) in this work are approx. 1-10 wt.%, with some cases slightly lower than 1% (two growth boundaries as to be discussed later.) After more than 70 temperature-pressure sets and 200 CVD run, we conclude that temperature and pressure are positively correlated in extended parametric window, i.e., decreasing ethanol pressure is necessary when synthesizing SWCNTs at lower temperatures. This strong dependence between

temperature and pressure was also noticed before in other system and therefore is probably universal in CVD synthesis of SWNTs. [22-24]

A systematic and comprehensive exploration on CVD conditions done in this work are presented in Fig. 5, in which one spot corresponds to one pair of temperature and pressure in CVD. In this counterplot, experimental temperature range is from 350°C to 950°C while pressure range is from 0.02 Pa to 14 kPa (Growth window of conventional ACCVD is shown as blue-line box for comparison). G/D ratios decided by Raman spectra (average value of four laser energies) are marked by different color/shapes and added on corresponding experimental conditions. By comparing these values of G/D ratio, we clearly observe a positive correlation between temperature and pressure. The effect of temperature and pressure on the quality of SWCNTs in expanded ACCVD system can be extracted from this counterplot.

Though efficient growth are achieved in a wide operation window (green region in Fig. 5), diameter and quality of the produced SWCNTs are strongly dependent on growth temperature and pressure, which affect the size of catalysts, growth rate, carbon feeding, etc. When pressure is fixed as 5 Pa, G/D ratio gradually decreased with decreasing temperature from over 50 (@850°C) to about 10 (@500°C). Growth of SWCNTs gradually terminate when temperature decreased to 400°C. From the characterization results in Fig. 1, low temperature also has effects on the diameter size of SWCNTs, which is probably due to the decreased size of catalyst nanoparticles at low temperatures. It can be further explained as that small size of catalyst nanoparticles or aggregators due to the decreased migration mobility of them at low temperatures lead to growth of small diameter SWCNTs.[25, 26] An interesting phenomenon was also identified during the characterization of SWCNTs growth from 500°C to 850°C at 5 Pa. Small diameter SWCNTs are hardly obtained

at high temperatures, it indeed observed that the growth of small diameter SWCNT reduced a lot from 500°C to 750°C, dominant chirality shift from small diameter SWCNTs (6,5) to relative large diameter SWCNTs (7,6), (8,6) and so on. However, when temperature is increased to 800°C, PL intensity of small diameter SWCNTs (6,5) and (8,3) become obviously enhanced again, and some weak signals can be detected for even super-small diameter SWCNTs such as (6,4) and (7,3). Broad diameter distribution of SWCNTs similar to HiPCo [27] is obtained at 800°C and 5 Pa. This trend is also concluded in Fig. S2, which presents the normalized PL intensity of (7,5), (6,5), (6,4) and so on. However, we emphasize there that PL has the limitation of not being able to detect metallic SWCNTs, which are also synthesized under this condition. This can be revealed by the broad G^- peak in BWF line shape of Raman spectra by 488 nm laser and 532 nm laser. Furthermore, absorption spectra shown in Fig. 3 identify the agreement with the trends that are concluded from results of Raman and PL.

Fig. 4a reveal increased diameter distributions with decreasing pressure, SWCNTs with broader diameter distribution are obtained at low pressure 0.1 Pa than that at 5 Pa. This phenomenon also happens when comparing the PL mapping of SWCNTs obtained here (750°C and 5 Pa) to that SWCNTs obtained in previous report (750°C and 1300 Pa), [19] SWCNTs with broader diameter distribution are obtained at low pressure 5 Pa than that at 1300 Pa. We assume that the carbon supply, which is proportional to the ethanol partial pressure, plays a critical role on the on the diameter distribution of SWCNTs. With proper carbon supply, broad diameter distribution of SWCNTs can be obtained. However, when the carbon supply is beyond the capacity of catalyst, over-loaded carbon will collide to form amorphous carbon then encapsulate or poison catalysts, which leads to a narrow diameter distribution of SWCNTs. This assumption of considering the influence from pressure as the effect of carbon supply on the growth of SWCNTs clarify the

agreement with other works. [28, 29] In addition, Fig. 5 also demonstrates that G/D is decreasing when pressure is increased from 0.1 Pa to 1300 Pa at 550°C. At this relative low temperature 550°C, SWCNTs are hardly obtained at 1300 Pa while good quality SWCNTs can be synthesized at 0.1 Pa. When temperature is stable, defect of SWCNTs is decreasing due to decreased pressure. Therefore, CVD pressure strongly effect on the diameter distribution and quality of SWCNTs.

According to the growth map in Fig. 5, growth boundary of SWCNTs can be identified by red crosses. There are two boundary areas, one is low temperature limit and the other is high temperature limit, both of which are dependent on ethanol pressure. Raman spectra in Fig. 4b also clearly track this growth trend, at a low pressure 0.02 Pa, no SWCNTs can be obtained at temperatures lower than 400°C or higher than 700°C. The best quality of SWCNTs is obtained at moderate temperature around 500°C. For this phenomenon, we believe SWCNTs cannot be grown at low temperatures possibly because of low growth rate of SWCNTs or the inactive catalyst (to further discuss later). The other interesting boundary, it cannot be observed the growth of SWCNTs at too high temperature and too low pressure (700°C and 0.02 Pa). However, this boundary has a dependence on CVD growth time, it shifts or disappear (Fig. S3) when CVD experimental time is elongated, suggesting a growth incubation at high temperature and low partial pressure. Therefore, this boundary is marked as dashed line in Fig. 5.
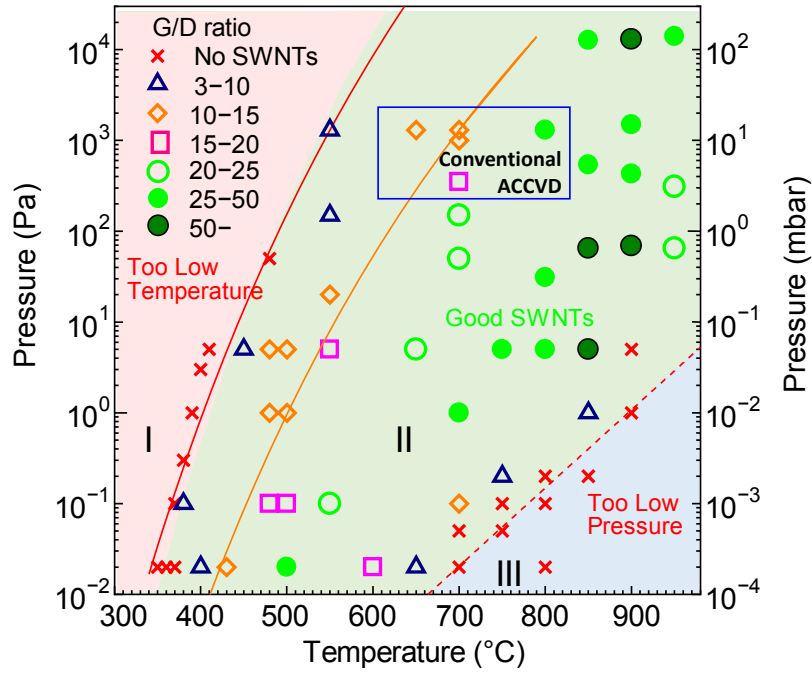
Figure 5. Counterplot of experimental map including all experimental information (temperature and pressure) done in extended ACCVD. Different G/D ratio measured by Raman are marked by different color; orange line is fitted by estimating activation energy as 2.3 eV. Growth window is divided into three regions (I, II, III highlighted in different colors), and blue box shows the parametric range studied in conventional ACCVD.

3.3 Strong temperature-pressure correlation from kinetic analysis

Kinetic study on the growth of SWCNTs well explains the strong dependence between temperature and pressure in extended ACCVD. Growth rate of SWCNTs can be considered proportional to $\exp\left(-\dfrac{E_a}{k_B T}\right)$, while the collision of carbon which is decided by number of density

or velocity proportional to $\dfrac{p}{T}\sqrt{T} = \dfrac{p}{\sqrt{T}}$. Where T is reaction temperature, P is pressure of ethanol,

E_a is total activation energy, and k_B is Boltzmann constant.

During the ACCVD growth of SWCNTs, there is a competition between the growth of SWCNTs and collision of carbon. In order to grow SWCNTs with a uniform quality, the ratio of reaction rate of SWCNTs to collision rate of carbon should be stable and exceed one critical value $C_{critical}$, expressed as:

$$\frac{\text{Reaction Rate}}{\text{Collision Rate}} = const > C_{critical} \qquad (1)$$

$$\frac{\sqrt{T}}{p}\exp\left(-\frac{E_a}{k_B T}\right) = const = \frac{\sqrt{T^*}}{p^*}\exp\left(-\frac{E_a}{k_B T^*}\right) > C_{critical} \qquad (2)$$

Where T* is another reaction temperature, P* is also another ethanol pressure. From equation (2), it is clearly revealed the positive correlation of pressure is necessary for optimal temperature to growth of stable SWCNTs. During the experimental observation, when we decreased the temperature, proper lower pressure is required. In Fig. 5, it also can be roughly concluded that the quality of SWCNTs (presented by G/D) is stable along a positive trend of temperature and pressure. Experimental results confirm the prediction of temperature and pressure by this simple kinetic model.

When we obtain uniform SWCNTs (constant G/D), equation (2) is rewritten as following equation (3) to fit the experimental results with uniform quality of SWCNTs, such as red line boundary between region I and II and orange line of 10<G/D<15.

$$p / p^* = \sqrt{\frac{T}{T^*}} \exp\left(-\frac{E_a}{k_B}\left(\frac{1}{T} - \frac{1}{T^*}\right)\right)$$

(3)

As shown by the orange line which covers six magnitude pressure range in Fig. 5, the activation energy is fitted to be 2.3 eV for growth of SWCNTs in this study (ethanol as carbon source and Co as catalyst). This value of activation energy is a little higher than other works [30, 31] because of the reasonable influence from secondary reaction of ethanol in gas-phase during ACCVD synthesis of SWCNTs, but is very close to the previous reported calculation for growth of SWCNTs with ethanol using Co as catalyst. [32] Growth boundary between region I and II is also fitted by 2.3 eV with solid red line in Fig. 5.

The physical meaning of this strong temperature and pressure is briefly discussed as follows. So far in our TEM investigations, amorphous carbon are seldom observed on ACCVD-produced SWNTs (possibly due to the etching effect of oxygen in an ethanol molecule). Therefore, we rule out the significant influence of amorphous carbon, and attribute the obtained G/D ratio to the intrinsic crystallization of product (i.e. proportion of defect in graphite lattice). In this context, a given density of defects correspond to a certain ratio between tube growth rate and carbon supply, and both insufficient carbon supply and over-loading result in the formation of more defects, which is reflected by the decreased G/D ratio at un-optimized conditions. Therefore, positive correlation between temperature and pressure is intrinsically the rate matching between carbon feeding and carbon precipitation, which well explains the general trend in the plot.
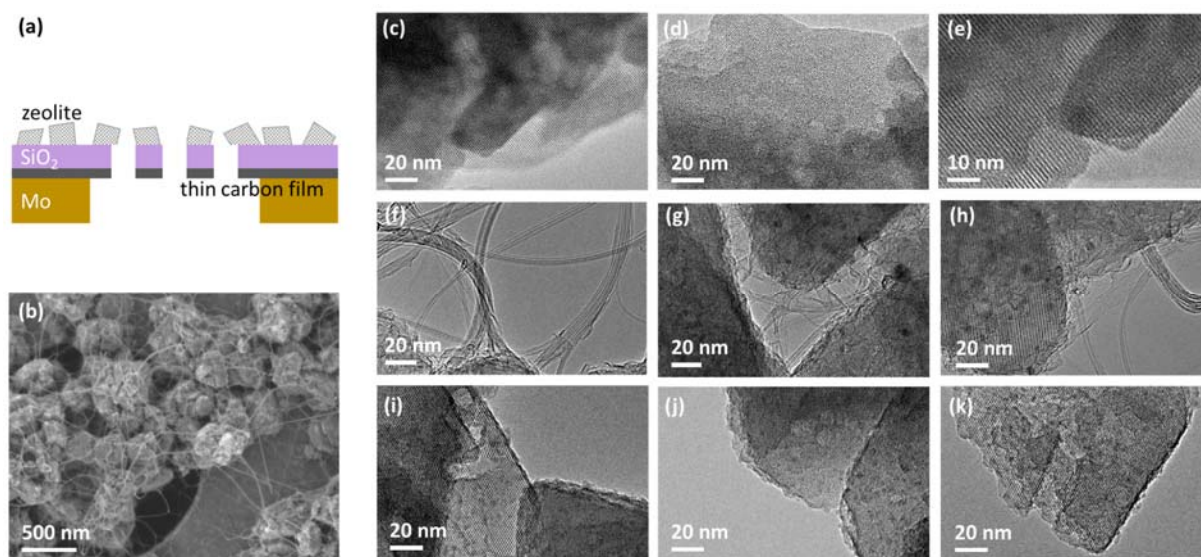
3.4 Growth boundaries from microscopic analysis

Figure 6. (a) Schematic and (b) SEM image of direct growth of SWCNTs on a SiO_2 coated Mo TEM grid, which allowed observation of zeolite-SWCNTs in original morphology without post-treatment or sample transfer. (c)-(k) Characteristic TEM images of zeolite-SWCNTs grown after different CVD conditions in an extended ACCVD plot (Fig. 3): (c)(d)(e) 0.02 Pa, 380°C (boundary of region I and II); (f)(g)(h) 15 kPa, 900°C (region II); (i)(j)(k) 0.02 Pa, 700°C (boundary of region II and III).

To further shed some lights on the growth mechanism from a microscopic view, we performed TEM characterization on SWCNT samples grown at different conditions. One uniqueness in this work is that we dispersed catalyst (FeCo supported on zeolite) onto a SiO_2 coated Mo TEM grid, which is stable at high temperatures (schematic shown in Fig. 6a). Therefore, SWCNTs are directly grown on this grid and used for TEM observation (SEM image shown in Fig. 6b). This strategy avoided complicated transfer process, and hence kept the samples in their original morphologies. Also, considering that zeolite is fragile under e-beam, a very weak electron dose is used during the entire measurement.

Fig. 6c-e show typical TEM images of one sample grown at 380°C with a pressure of 0.02 Pa (boundary between region I and II in Fig. 5). The periodic channels of zeolite can be clearly seen, while no noticeable SWCNT-like structures are observed. In comparison, a sample grown in region II (efficient growth) is shown in Fig. 6f-h, where abundant SWCNTs clearly exist. One interesting phenomenon in Fig 6c-e is that no catalyst particles are observable on (or inside) zeolite. This possibly suggests the inefficient growth of SWCNTs is due to the difficulties in forming nanoparticles at this low temperature, e.g. reducing oxide catalyst precursor into metal. Considering this boundary depends on pressure, we speculate at this boundary ethanol first needs to reduce catalyst to form nanoparticles before forming a SWCNT. Therefore, in addition to the kinetic model discussed in the previous section, growth at a boundary condition possibly involve more complicated processes that are beyond the discussion of kinetic model. In this case, in addition to the possible over coating of catalyst (predicted by kinetic model), difficulties in reduction of catalyst precursor, aggregation of atoms into nanoparticles are also contributing to this first boundary between region I and II in Fig. 5.

One other sample grown at 700°C with a pressure of 0.02 Pa (boundary between region II and III) shows a very different morphology. Nanoparticles from 2-5 nm clearly exist in Fig. 6i-k. Though no tubular structure is observed, carbon coating are noticeable on particles at edges of a zeolite. Apparently there are no difficulties in reducing catalyst and forming nanoparticles. In contrast, it is possible that the metal atoms are highly mobile so that aggregate into larger particles before sufficient carbon comes for SWCNT nucleation. This explains why higher ethanol pressure or elongated growth time to increase carbon supply are needed for SWCNT growth in Fig. 5. Meanwhile, since the temperature is higher in this boundary, we begin to observe collapse of zeolite structure in Fig. 6i-k. Therefore, besides the insufficient carbon supply during fast particle

growth predicted by kinetic model, instability of zeolite at high temperatures could be also responsible for inefficient growth for this second boundary between region II and III.

3.5 Super-small diameter SWCNTs thinner than (6,5)

During the exploration of expanded ACCVD growth of SWCNTs, the efficient growth and observation of super-small diameter SWCNTs (<~1 nm) is an important achievement besides the fundamental understanding on the growth mechanism. Characterization of super-small diameter SWCNTs is discussed here in detail.

Raman spectra of SWCNTs synthesized at a temperature of 500°C and a pressure of 5 Pa were shown previously in Fig. 1, Raman spectra by four laser lines present an obvious up-shift comparing to the SWCNTs synthesized at high temperatures, which means smaller diameter SWCNTs can be obtained at low temperature and low pressure conditions. Identified assignments [33, 34] of Raman can be found in Fig. S3. In Raman spectra S3, the peaks appeared at high frequency observed by 532 nm laser in this work are demonstrated as (7,3) and (6,5). (6,4) and (8,0) are determined by 633 nm, (9,1) and (5,4) are observed by 785 nm laser, and (7,4) is observed by 488 nm laser, respectively. Rarely used laser 1064 nm also indicates small diameter SWCNTs ($d_t < 1$ nm) (7,6), (8,4) and (9,2). All assigned SWCNTs with super-small diameter (optical band gap up to ~1.5 eV) are shown in Table 1. Each SWCNT with corresponding Raman shift is shown in this table.

(n,m)	d_t (nm)	ω_{RBM}				
		λ_{1064nm}	λ_{785nm}	λ_{633nm}	λ_{532nm}	λ_{488nm}
(5,4)	0.620		370.35			
(8,0)	0.635			361.85		
(6,4)	0.692			331.88		
(7,3)	0.706				331.40	
(6,5)	0.757				303.69	
(9,1)	0.757		303.62			
(7,4)	0.765					304.85
(8,3)	0.782			294.54		
(9,2)	0.806	286.76			286.31	
(7,5)	0.829			280.31		
(8,4)	0.840	277.21				
(7,6)	0.895	259.97		260.85		
(7,7)	0.963					242.08
(8,7)	1.032		232.11			

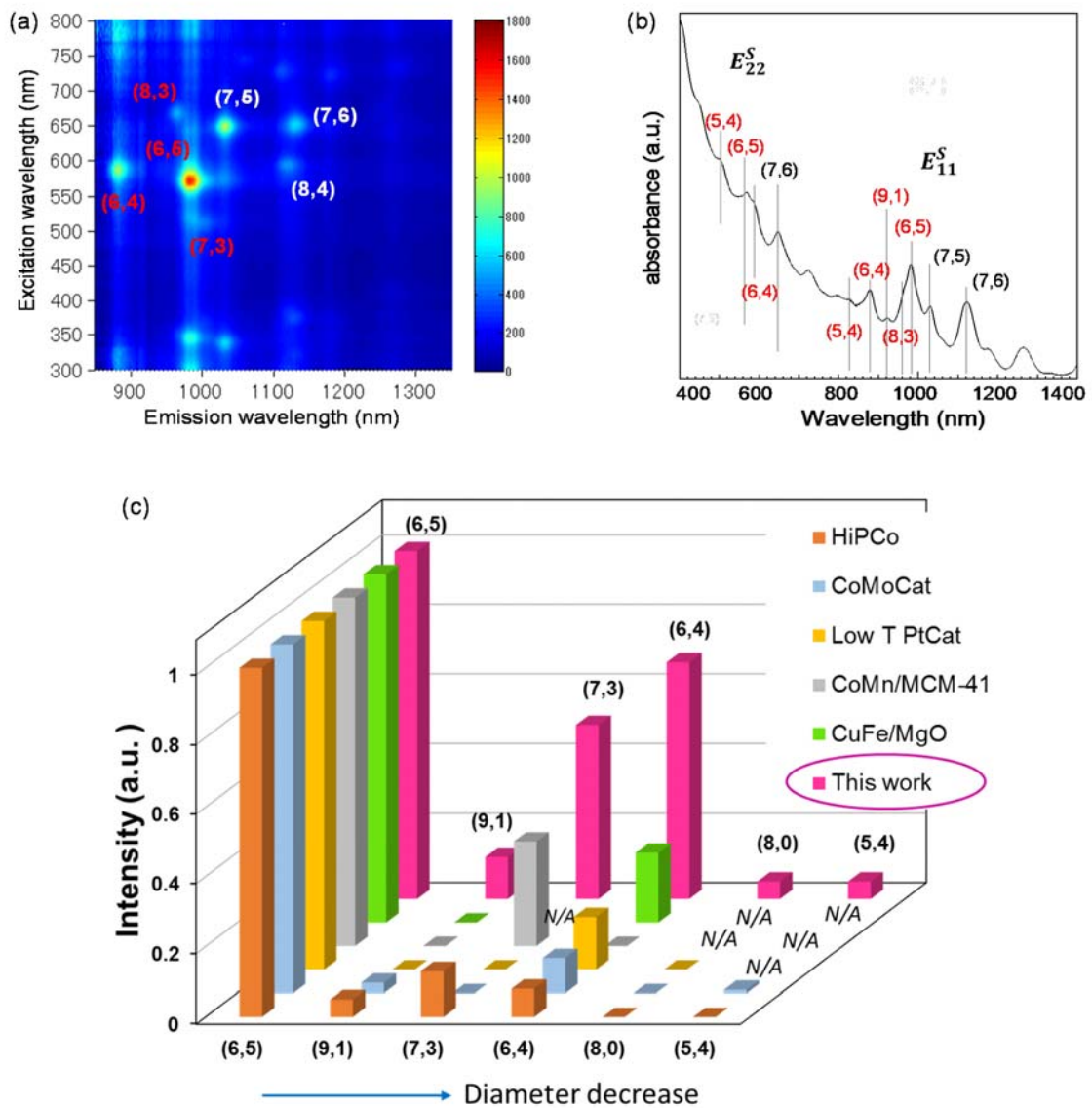**Table 1**. Chiral index of small diameter SWCNTs identified by Raman.

Figure 7. Assignments of SWCNTs growth at low temperature and pressure by (a) PL, (b) absorption spectra. (c) Comparison of small diameter SWCNTs observed between previous works and this work [27, 35-38]

Semiconducting SWCNTs are observed by PL, as shown in Fig. 7a. (6,5) becomes dominant in as-grown sample, together with relative high concentration (6,4), (7,5) and so on. It has a good

agreement with RBM of Raman to identify the chirality of SWCNTs, for example, (7,5), (7,6), (6,4) and (8,3) observed by 633 nm laser and (6,5), (7,3) observed by 532 nm laser in Raman. (5,4) which has strong Raman resonance signal by 785 laser also can be observed by PL as shown in Fig. S4. Optical absorption spectra in Fig. 7b with transition energies E_{11} and E_{22} are also in good agreements with PL results.

These super-small diameter SWCNTs efficiently enhanced in this work were rarely obtained from direct growth in previous reports. For example, (6,4) was usually extracted from inner tube of a double-walled carbon nanotubes. [39, 40] Only a few studies reported the observation of small diameter which is thinner than (6,5). As shown in Fig. 7c, the ratio of (6,4) to (6,5) is roughly determined by the intensity of PL, almost 60% is achieved by this work. In other works, the ratio of (6,4) to (6,5) is around 10%,[27, 35, 38, 41] even in some work that obtained small diameter ~0.6 nm, data of (6,4) cannot found in all PL maps. [36] Only in one recent report of (6,5) predominant work, this ratio increased to ~20% estimate by PL intensity. [37] Our work reveals an excellent efficiency not only for the relative amount but also the varieties of super-small diameter SWCNTs as one of the most efficient work to achieve the growth of super-small diameter SWCNTs thinner than (6,5), which is resulted from the successful extension of growth parameter window in ACCVD. These SWCNTs with small diameter and high crystallization are expected to be useful in photo-electronic device. Being able to efficiently grow SWCNTs in a such wide range of CVD parameters is also expect to make growth compatible to more processes, and to extend the potential applications of SWCNTs to other fields.

4. CONCLUSIONS

We performed a comprehensive parametric study on alcohol catalytic chemical vapor deposition (ACCVD) synthesis of single-walled carbon nanotube, systematically varied temperature range from 340 to 950°C and pressure over 6 order magnitudes. With more than 70 temperature-pressure sets, we present a counterplot of temperature and pressure which we name extended ACCVD map. In this extended ACCVD high quality SWCNTs were efficiently synthesized at temperatures lower than 400°C combining with partial pressure of ethanol as low as 0.02 Pa. Particularly, the ratio of smaller diameter tubes was significantly increased and super-small diameter SWCNTs (0.8 nm > d_t > 0.52 nm) were obtained in the expanded ACCVD. Resonant Raman with five excitation laser lines, UV-vis-NIR optical absorption, and photoluminescence (PL) are used to characterize the abundance of small diameter nanotubes, and chirality of super-small diameter SWCNTs thinner than (6,5) were assigned as (6,4), (5,4), (7,3), and (8,0). Besides, growth mechanism of SWCNTs in extended ACCVD is clarified through a kinetic model on the experimental map and investigated by a transfer-free TEM observation of catalysts and as-grown SWCNTs. We believe this work refreshed our previous understanding of ACCVD, and enabled synthesis of high quality SWCNTs at extreme, e.g. ultra-low temperature or pressure, conditions.

ACKNOWLEDGMENT

SUPPORTING INFORMATION AVAILABLE

CVD apparatus; Intensity for specific chirality of dispersed SWCNTs growth from 800°C to 500°C at 5 Pa; Growth time dependence of G band by Raman at 700°C and 0.02 Pa; Assignments of obtained SWCNTs at 500°C and 5 Pa by Raman spectra (5 lasers) coupling with Kataura plot; PL map indicates (5,4) and (6,4) in SWCNTs obtained at 500°C, 5 Pa.

REFERENCES

1. Jorio, A; Dresselhaus, M. S; Dresselhaus, G. Carbon nanotube: Advanced topics in the synthesis, structure, properties and application. *Topics in applied physics* 111, **2008**

2. Yang, F.; Wang, X.; Li, M.H.; Liu, X. Y.; Zhao, X. L.; Zhang, D. Q.; Zhang, Y.; Yang, J.; Li, Y. Templated synthesis of single-walled carbon nanotubes with specific structure. *Acc. Chem. Res.* **2016**, 49, 606–615

3. Zhang, Q.; Huang, J.Q.; Qian, W. Z.; Zhang, Y. Y.; Wei, F. The road for nanomaterials industry: A review of carbon nanotube production, post-treatment, and bulk applications for composites and energy storage. *Small* **2013**, 9 (8), 1237–1265

4 Liu, C.; Cheng, H. M. Controlled growth of semiconducting and metallic single-wall carbon nanotubes. *J. Am. Chem. Soc.* **2016**, 138 (21), 6690–6698.

5. Bethune, D. S.; Kiang, C. H.; Vries, M. D.; Gorman, G.; Savoy, R.; Vazquez, J.; Beyers, R. Cobalt-catalysed growth of carbon nanotubes with single-atomic-layer walls. *Nature* **1993**, 363, 605-607

6. Thess, A.; Lee, R.; Nikolaev, P.; Dai, H. J.; Petit, P.; Robert, J.; Xu, C. H.; Lee, Y. H.; Kim, S. G.; Rinzler, A. G.; Colbert, D. T.; G. Scuseria, E.; Tomanek, D.; Fischer, J. E.; Smalley, R. E. Crystalline ropes of metallic carbon nanotubes. *Science* **1996**, 273, 483-487

7. Kong, J.; Soh, H.; Casssell, A.; Quate, C. F.; Dai, H. Synthesis of individual single-walled carbon nanotubes on patterned silicon wafers. *Nature* **1998**, 395, 878-881

8. Nikolaev, P.; Bronikowski, M. J.; Bradley, R. K.; Rohmund, F.; Colbert, D. T.; Smith, K. A.; Smalley, R. E. Gas-phase catalytic growth of single-walled carbon nanotube from carbon monoxide. *Chem. Phys. Lett.* **1999**, 313, 91-97

9. Li, Y. M.; Mann, D.; Rolandi, M.; Kim, W.; Ural, A.; Hung, S.; Javey, A.; Cao, J.; Wang, D. W.; Yenilmez, E.; Wang, Q.; Gibbons, J. F.; Nishi, Y.; Dai, H. J. Preferential growth of semiconducting single-walled carbon nanotubes by a plasma enhanced CVD method. *Nano Lett*. **2004**, 4, 317-321

10. Maruyama, S.; Kojima, R.; Miyauchi, Y.; Chiashi, S.; Kohno, M. Low-temperature synthesis of high-purity single-walled carbon nanotubes from alcohol. *Chem. Phys. Lett.* **2002**, 360, 229-234

11. Murakami, Y.; Chiashi, S.; Miyauchi, Y.; Hu, M.; Ogura, M.; Okubo, T.; Maruyama, S. Growth of vertically aligned single-walled carbon nanotube films on quartz substrates and their optical anisotropy. *Chem. Phys. Lett.* **2004**, 385, 298-303

12. Xiang, R.; Einarsson, E.; Okawa, J.; Miyauchi, Y.; Maruyama, S. Acetylene-accelerated alcohol catalytic chemical vapor deposition growth of vertically aligned single-walled carbon nanotubes. *J Phys Chem C* **2009**, 113, 7511-7515.

13. Chiashi, S.; Okabe, H.; Inoue, T.; Shiomi, J.; Sato, T.; Kono, S.; Terasawa, M.; Maruyama, S. Growth of horizontally aligned single-walled carbon nanotubes on the singular R-plane (10-11) of quartz. *J. Phys. Chem. C* **2012**, 116, 6805-6808

14. Inoue, T.; Hasegawa, D.; Badar, S.; Aikawa, S.; Chiashi, S.; Maruyama, S. Effect of Gas pressure on the density of horizontally aligned single-walled carbon nanotubes grown on quartz substrates. *J. Phys. Chem.* **2013**, 117-22, 11804-11810

15. Cui, K.; Anisimov, A. S.; Chiba, T.; Fujii, S.; Kataura, H.; Nasibulin, A. G.; Chiashi, S.; Kauppinen, E. I.; Maruyama, S. Air-stable high-efficiency solar cells with dry-transferred single-walled carbon nanotube films. *J. Mater. Chem. A* **2014**, 2, 11311-11318

16. Cui, K.; Chiba, T.; Omiya, S.; Thurakitseree, T.; Zhao, P.; Fujii, S.; Kataura, H.; Einarsson, E.; Chiashi, S.; Maruyama, S. Self-assembled micro-honeycomb network of single-walled carbon nanotubes for solar cell. *J. Phys. Chem. Lett.* **2013**, 4, 2571-2576

17. Aikawa, S.; Xiang, R.; Einarsson, E.; Chiashi, S.; Shiomi, J.; Nishikawa, E.; Maruyama, S. Facile fabrication of all-SWNT field-effect transistors. *Nano Res.* **2011**, 4-6, 580-588

18. Murakami, Y.; Miyauchi, Y.; Chiashi, S.; Maruyama, S. Characterization of single-walled carbon nanotubes catalytically synthesized from alcohol. *Chem. Phys. Lett.* **2003**, 374, 53-58

19. Miyauchi, Y.; Chiashi, S.; Murakami, Y.; Hayashida, Y.; Maruyama, S. Fluorescence spectroscopy of single-walled carbon nanotubes synthesized from alcohol. *Chem. Phys. Lett.,* **2004**, 387(1-3), 198-203

20. Igarashi, H.; Murakami, H.; Murakami, Y.; Maruyama, S.; Nakashima, N. Purification and characterization of zeolite-supported single-walled carbon nanotubes catalytically synthesized from ethanol. *Chem Phys Lett* **2004**, 392, 529-532

21. Xiang, R.; Wu, T. Z.; Einarsson, E.; Suzuki, Y.; Murakami, Y.; Shiomi, J.; Maruyama, S. High-precision selective deposition of catalyst for facile localized growth of single-walled carbon nanotubes. *J Am Chem Soc* **2009**, 131, 10344-10345

22. Futaba, D. N.; Hata, K.; Yamada, T.; Mizuno, K.; Yumura,M.; Iijima, S. Kinetics of water-assisted single-walled carbon nanotube synthesis revealed by a time-evolution snalysis. *Phys. Rev. Lett.* **2005,** 95, 056104 1-4

23 Picher, M.; Anglaret, E.; Arenal, R.; Jourdain, V. Self-deactivation of single-walled carbon nanotube growth studied by in situ Raman measurement. *Nano letters* **2009**, 9 (2), 542-547

24 Maruyama, T.; Kondo, H.; Ghosh. R.; Kozawa, A.; Naritsuka, S. Iizumi, Y.; Okazaki, T.; Iijima, S. Single-walled carbon nanotube synthesis using Pt catalysts under low ethanol pressure via cold-wall chemical vapor deposition in high vacuum. *Carbon* **2016**, 9, 6-13

25. Li, N.; Wang, X.; Ren, F.; Haller, G. L.; Pfefferle, L. D. Diameter tuning of single-walled carbon nanotubes with reaction temperature using a Co monometallic catalyst. *J. Phys. Chem. C* **2009**, 113(23), 10070-10078

26. Fukuoka, N.; Mizutani, Y.; Naritsuka, S.; Maruyama, T.; Iijima, S. Low-temperature synthesis of single-walled carbon nanotubes in a high vacuum using Pt catalyst in alcohol gas source method. *Jpn. J. Appl. Phys.* **2012**, 51, 06FD23 1-4

27. Bachilo, S. M.; Strano, M. S.; Kittrell, C.; Hauge, R. H.; Smalley, R. E.; Weisman*,* R. B. Structure-assigned optical spectra of single-walled carbon nanotubes. *Science* **2002**, 298, 2361-2366

28. Wang, B.; Poa, C. H. P.; Wei, L.; Li, L. J.; Yang, Y.; Chen, Y. (*n,m*) Selectivity of single-walled carbon nanotubes by different carbon precursors on Co−Mo Catalysts. *J. Am. Chem. Soc.* **2007**, *129* (29), 9014-9019

29. Maruyama, T.; Kondo, H.; Fukuoka, N.; Naritsuka, S. Growth of Single-Walled Carbon Nanotubes from Pt catalysts by the alcohol gas source method under low ethanol pressure: growth temperature dependence. *trans. mat. res. soc. japan* **2013**, 38 (4), 585-588

30. Wirth, C.T.; Zhang, C.; Zhong, G.; Hofmann, S.; Robertson, J. Diffusion and reaction limited growth of carbon nanotube forests. *ACS nano*, **2009**, 3, 3560-3566

31. Einarsson, E.; Murakami, Y.; Kadowaki, M.; Maruyama, S. Growth dynamics of vertically aligned single-walled carbon nanotubes from *in situ* measurements. *Carbon* **2008**, 46, 923-930

32. Vinten, P.; Lefebvre, J.; Finni, P. Kinetic critical temperature and optimized chemical vapor deposition growth of carbon nanotubes. *Chem. Phys. Lett.* **2009**, 469, 293-297

33. Kataura, H.; Kumazawa, Y.; Maniwa, Y.; Umezu, I.; Suziki, S.; Ohtsuka, Y.; Achiba, Y. Optical properties of single-wall carbon nanotubes. *Synthesis Metals* **1999**, 103, 2555-2558

34. Araujo, P. T.; Doorn, S. K.; Kilina, S.; Tretiak, S.; Einarsson, E.; Maruyama, S.; Chacham, H.; Pimenta, M. A.; Jorio, A. The third and fourth optical transitions in semiconducting carbon nanotubes. *Phys. Rev. Lett.* **2007**, **9**8, 067401-1-067401-4

35. Maruyama, T.; Mizutani, Y.; Naritsuka, S.; Iijima, S. Single-walled carbon nanotube growth in high vacuum using Pt catalyst in alcohol gas source method. *Materials Express* **2011**, 1, 267-272

36. Loebick, C. Z.; Derrouiche, S.; Marinkovic, N.; Wang, C.; Hennrich, F.; Kappes, M. M.; Haller G. L.; Pfefferle, L. D. Effect of manganese addition to the Co-MCM-41 catalyst in the selective synthesis of single wall carbon nanotubes. *J. Phys. Chem. C* **2009**, 113, 21611-21620

37. He, M.; Chernov, A. I.; Fedotov, P. V.; Obraztsova, E. D.; Sainio, J.; Rikkinen, E.; Jiang, H.; Zhu, Z.; Tian, Y.; Kauppinen, E. I.; Niemela M.; Krause, A. O. I. Predominant (6, 5) single-walled carbon nanotube growth on a copper-promoted iron catalyst. *J. Am. Chem. Soc.* **2010,** 132, 13994-13996

38. Bachilo, S. M.; Balzano, L.; Herrera, J. E.; Pompeo, F.; Resasco, D. E.; Weisman, R. B. Narrow (*n,m*)-Distribution of single-walled carbon nanotubes grown using a solid supported catalyst. *J Am Chem Soc* **2003**, 125,11186-11187

39. Miyata, Y.; Suzuki, M.; Fujihara, M.; Asada, Y.; Kitaura, R.; Shinohara, H. Solution-phase extraction of ultrathin inner shells from double-wall carbon nanotubes. *ACS Nano* **2010**, 4, 5807-5812

40. Shiozawa, H.; Kramberger, C.; Pfeiffer, R.; Kuzmany, H.; Pichler, T.; Liu, Z.; Suenaga, K.; Kataura, H.; Silva, S.R.P. Catalyst and chirality dependent growth of carbon nanotubes determined through nano-test tube chemistry. *Advanced Materials* **2010**, 22, 3685-3689

41. Kavan, L.; Frank, O.; Green, A. A.; Hersam, M. C.; Koltai, J.; Zólyomi, V.; Kürti, J.; Dunsch, L. In situ Raman spectroelectrochemistry of single-walled carbon nanotubes: Investigation of materials enriched with (6,5) tubes. *J. Phys. Chem. C* **2008**, 112, 14179-14187
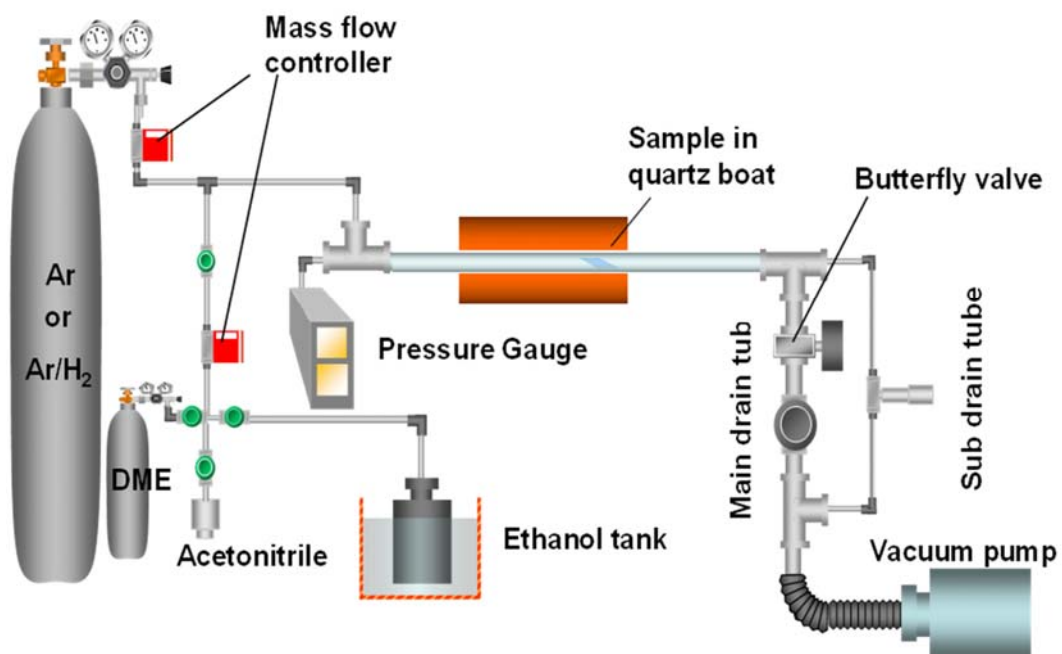
SUPPORTING INFORMATION

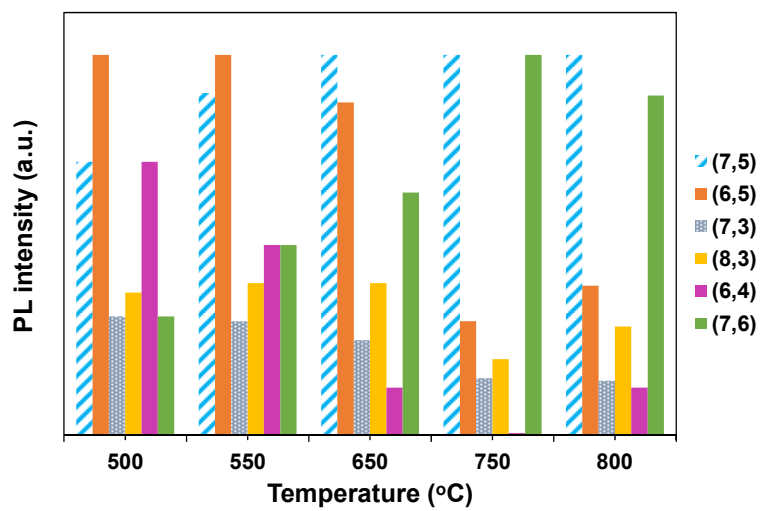**Figure S1 A schematic of** CVD apparatus used for ACCVD.

Figure S2 Intensity for specific chirality of dispersed SWCNTs growth at 800°C to 500°C with an ethanol pressure of 5 Pa.
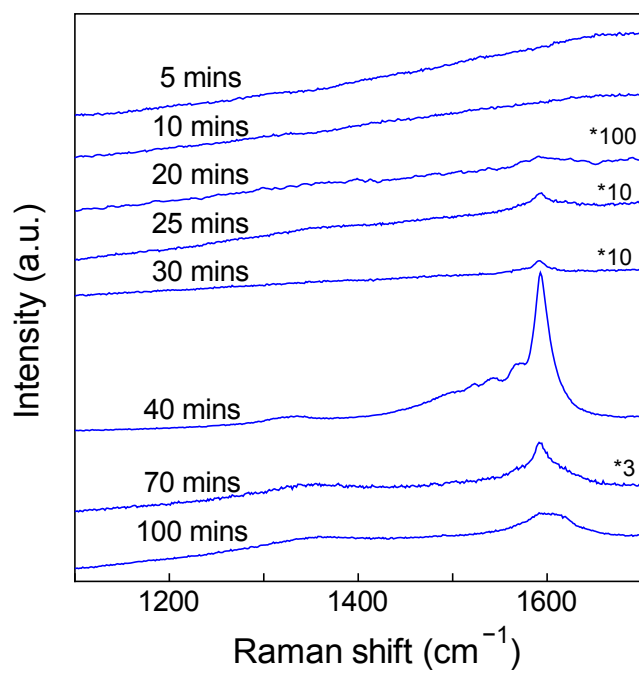
Figure S3 Growth time dependence of G band by Raman at 700°C and 0.02 Pa, revealing

growth of SWCNTs depends on the proper incubation time of carbon supply at low
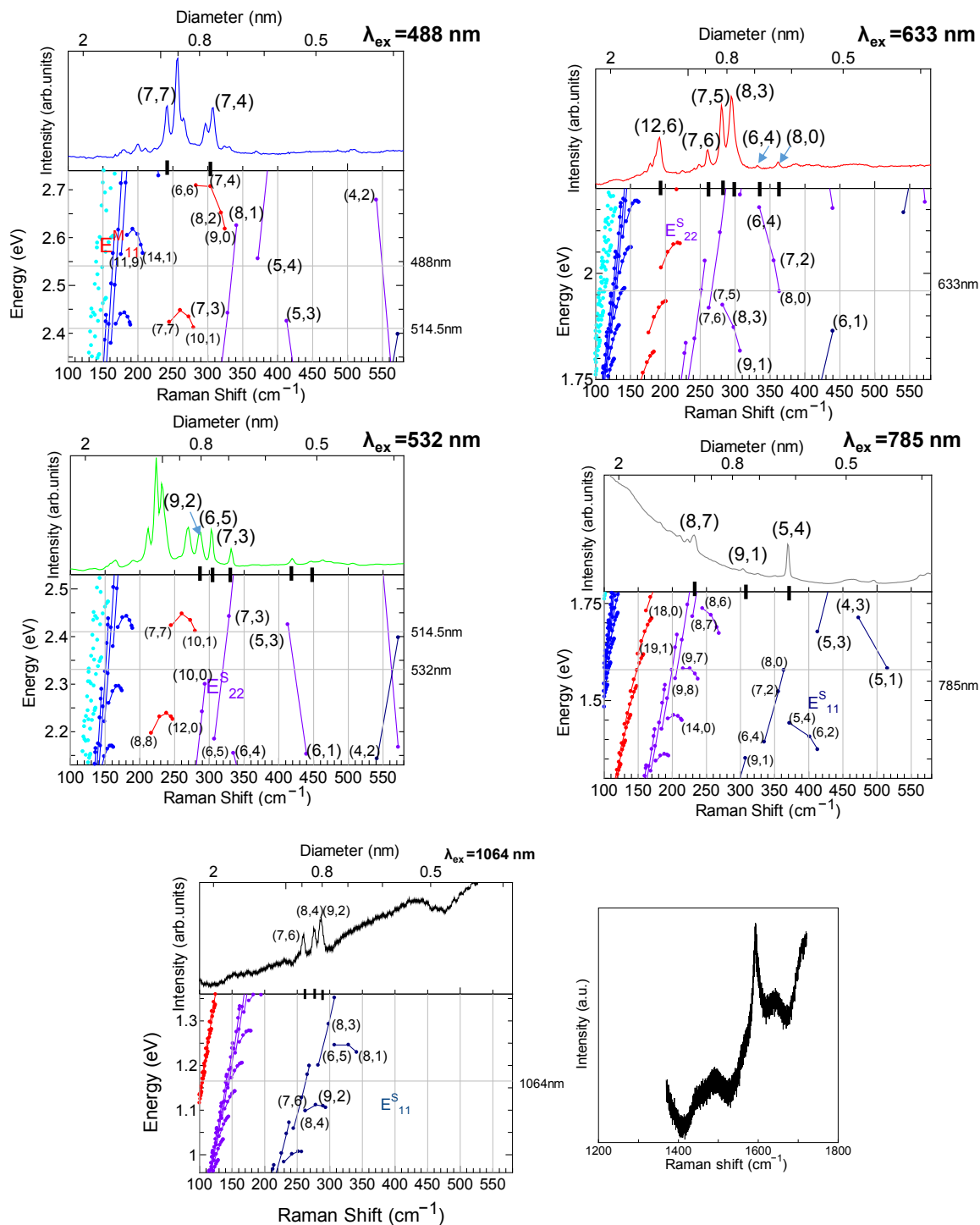
pressure condition

Figure S4 Assignments of SWCNTs growth at low temperature and pressure by Raman

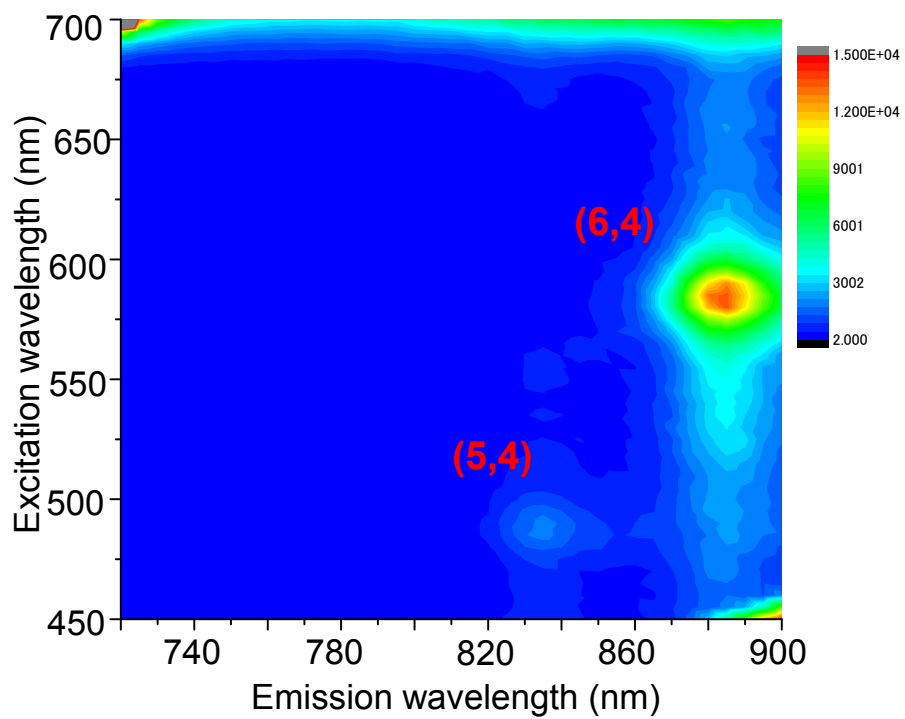spectra accompanied with Kataura plot, five different excitation energies were used.

Figure S5 PL map of SWCNTs obtained at 500°C, 5 Pa, confirming the existence of (5,4) and (6,4) SWCNTs.